carbides lying in the plane of the boundary; hence cavities tend to contain a number of carbides.

The minimum critical radius of a cavity is dependent on the applied stress through the equation $r = 2\gamma/\sigma$ [3], where r = cavity radius, γ = surface energy and σ = applied stress. There have been no cases reported [8] of cavities being observed having radii smaller than that given by the above equation, since below this value surface tension forces would be too strong to permit the cavity to remain. The minimum radius is not only dependent on the applied stress but also on the material, i.e. in Cu, Mg typical minimum radii of $\sim 0.3\,\mu m$, are observed whereas for high creep resistant alloys such as low alloy ferritic steels, the minimum radii can be as small as $0.01\,\mu m$. In the present case, taking $\gamma = 2\,Jm^{-2}$ and $\sigma = 135\,MN\,m^{-2}$, then the minimum cavity radius is $0.015\,\mu m$. Hence, the sub-micron cavities observed in Fig. 1 have just grown to above the minimum radius.

In conclusion, the observations show that it is possible to observe sub-micron cavities using SEM techniques and that in the low alloy steel studied nucleation occurs continuously and preferentially at grain boundary carbides by a process of decohesion of the carbide–matrix interface.

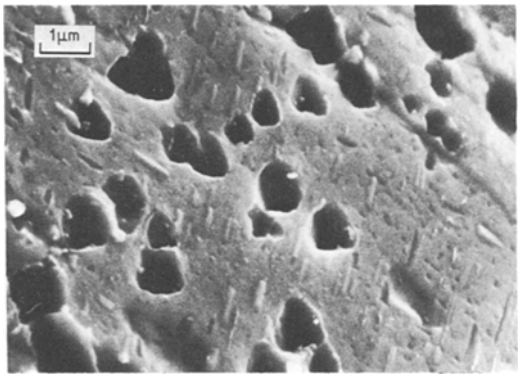

Figure 2 Grain boundary cavities enveloping carbides during growth in a 1.5% Cr–0.5% V low alloy steel after 1.5% strain at 650° C.

References

1. A. J. PERRY, *J. Mater. Sci.* **9** (1974) 1016.
2. R. G. FLECK, D. M. R. TAPLIN and C. J. BEEVERS, *Acta Met.* **23** (1975) 415.
3. J. E. HARRIS, *Trans AIME* **233** (1965) 1509.
4. B. F. DYSON, M. S. LOVEDAY and J. M. RODGERS, *Proc. Roy. Soc. London* **A349** (1976).
5. B. R. KIRBY and C. J. BEEVERS, *J. Mater. Sci.* **12** (1977) 1917.
6. D. A. MILLER and R. PILKINGTON, *Met. Trans.* (in press).
7. R. H. BUKALIL, C. ROQUES-CARMES, R. TIXIER, M. AUCOUTURIER and P. LACOMBE, *Met. Sci. J.* **8** (1974) 387.
8. G. W. GREENWOOD, "Fracture", Vol. 1 (University of Waterloo Press, Canada, 1977) p. 293.

Received 31 January
and accepted 10 March 1978.

D. A. MILLER*
R. PILKINGTON
Department of Metallurgy,
University of Manchester,
Manchester, UK

*Now at Department of Materials Science, University of Southern California, Los Angeles, California 90007, USA.

Anodic oxidation of InP and the quaternary alloy $Ga_xIn_{1-x}As_yP_{1-y}$

The full potential of semiconductor materials in the fabrication of electronic devices based on planar configurations may only be realized if suitable methods are available to form insulating oxide layers of acceptable qualities on their surfaces. Early work had relied on gas phase oxidation [1] but recently, following the work of Spitzer *et al.* [2], Hasegawa *et al.* [3, 4] and Hasegawa and Hartnagel [5] on the anodic oxidation of GaAs, electrochemical techniques with high electrolyte stability, reliability of procedure free from severe contamination effects and excellent reproducibility have become important. Accordingly, in a solution consisting of 3 wt% aqueous solution of tartaric acid mixed with propylene glycol (PGT), glass-like oxide films of thickness up to about 8000 Å may be grown on n-type GaAs in a few minutes. Factors such as electrolyte composition, pH, anodization current density and surface illumination decide the thickness and conductivity of the layers formed. In this

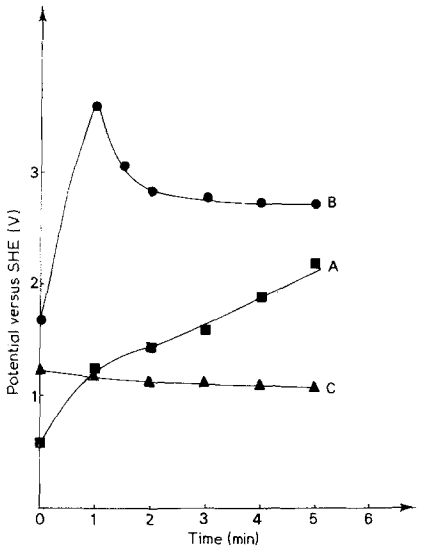

Figure 1 Potential–time dependences for (1 0 0) faces of n-n-type InP (A) in NaOH, pH = 9.5, at current density of 0.42 mA cm^{-2}; (B) in Na_2SO_4 pH = 7, at current density of 2 mA cm^{-2}; (C) in H_2SO_4, pH = 1.6, at current density of 2 mA cm^{-2}.

communication we describe preliminary aspects of our work, which is designed to extend the use of anodic oxidation to the preparation of oxides on the various crystallographic faces of n-type InP and on (1 1 1) epitaxially grown layers of the new quaternary semiconductor system, $Ga_xIn_{1-x}As_yP_{1-y}$ [6]. We focus attention on the importance of the various factors which control the anodic oxidation behaviour and present the morphological features of the oxide films formed under galvanostatic conditions. Both the chemical composition and the crystallographic properties of the oxide films at various stages in their growth will be described in future publications from this laboratory.

The anodic oxides were grown galvanostatically employing standard electrochemical procedures and apparatus [7]. Potential changes, referred to a standard hydrogen electrode, were recorded as a function of time and the oxide layers were examined by scanning electron microscopy (Cambridge Steroscan). The semiconductors, which were all n-type (carrier concentration about 1.0×10^{17} cm^{-3}, were fitted with In–Ga "ohmic" contacts and all materials and solutions were of the highest commercially available purity with the water triply-distilled and de-ionized. Illumination of the semiconductor surfaces in contact with the electrolytes was performed using a 100 W tungsten lamp.

Fig. 1 shows potential–time curves for the galvanostatic oxidation of (1 0 0) surfaces of n-type InP in different electrolytes. Increases in the potential with time, as is apparent for the dependence in NaOH (pH 9.5) – Curve A – are typical of the formation of an ion-conducting oxide layer [7], whereas decreases in potential with time similar to that observed in Na_2SO_4

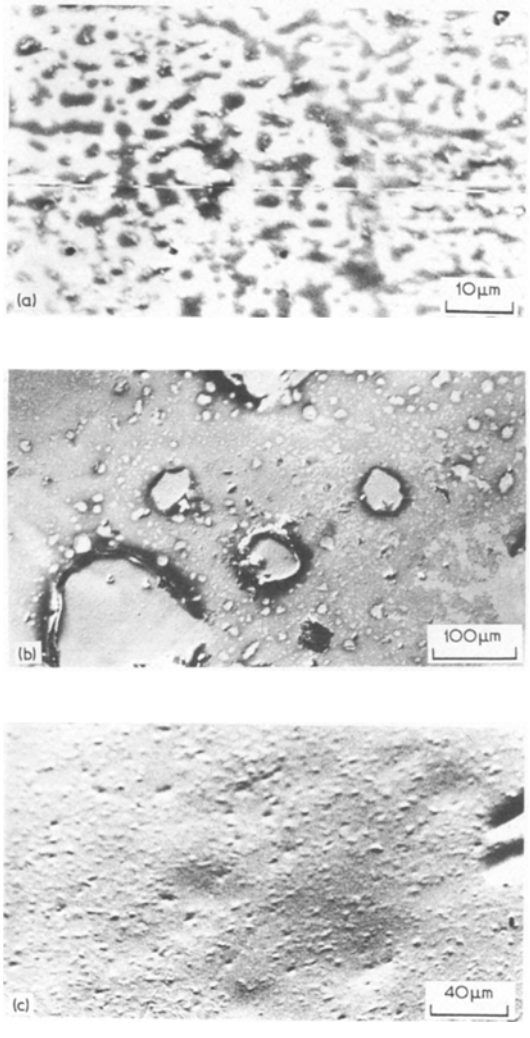

Figure 2 Scanning electron micrographs of (1 0 0) surfaces of InP following anodization: (a) for 2 min in PGT, pH = 9.5, at current density of 0.2 mA cm^{-2}; (b) for 5 min in PGT, pH = 2.5, at current density of 0.2 mA cm^{-2}; (c) for 15 min in H_2SO_4, pH = 1.6, at current density of 2.0 mA cm^{-2}.

(pH 7) – Curve B – may be taken as representing dissolution of the rapidly formed oxide layer. At low pH values, as in sulphuric acid – Curve C – no oxide layer formation is indicated from the potential–time dependence at a current density of $2\,mA\,cm^{-2}$. This type of analysis is confirmed in the scanning electron microscopic study of the surfaces. Fig. 2 shows the surfaces following galvanostatic anodization in PGT electrolytes of various pH values. At high pH values (Fig. 2a) what appears to be an amorphous oxide layer is formed after two minutes with a current density of $0.2\,mA\,cm^{-2}$, whereas at a pH of 2.5 (Fig. 2b) dissolution of the oxide layer has clearly followed the oxidation after five minutes at a current density of $0.2\,mA\,cm^{-2}$. At very low pH in sulphuric acid (Fig. 2c) no oxide layer has formed even after fifteen minutes anodization at $2\,mA\,cm^{-2}$. This micrograph coresponds to the situation described by Curve C of Fig. 1.

The behaviour of the various crystallographic faces of InP upon anodization in PGT electrolyte of pH = 5.9 at 290 K and a current density of $0.2\,mA\,cm^{-2}$, both in the absence and in the presence of illumination, is shown in Fig. 3. For each of the three crystallographic faces (1 1 1), (1 0 0) and (1 1 0) in the dark, the potential increases with time, signifying the slow formation of an oxide layer, which after about 5 min is

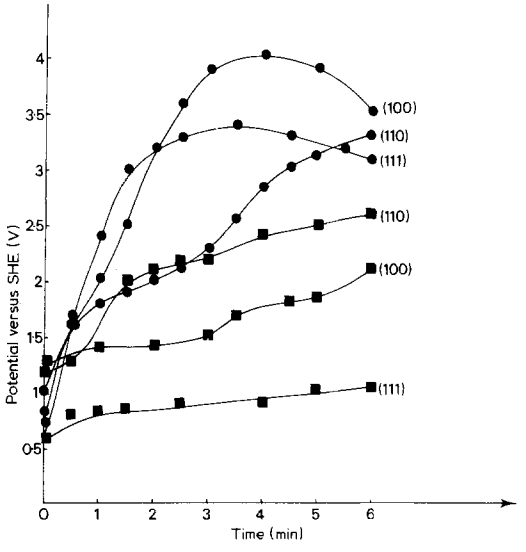

Figure 3 Potential–time dependences showing the effect of illumination on (1 0 0), (1 1 1) and (1 1 0) surfaces of InP with anodization in PGT, pH = 5.9, at a current density of $0.2\,mA\,cm^{-2}$. • in light; ▪ in dark.

Figure 4 Scanning electron micrograph showing oxide nucleii on (1 1 1) surface of InP following anodization in PGT, pH = 9.4, at a current density of $0.16\,mA\,cm^{-2}$.

estimated to be about 1000 Å thick in each case. Upon illumination the behaviour for (1 1 1) and (1 0 0) surfaces is quite different, exhibiting a rapid rise of potential with time followed by a plateau region, and then a decrease. Such behvaiour represents a fast oxidation process followed later by dissolution of the oxide layer. For a satisfactory oxide layer, therefore, under these conditions anodization must be terminated on (1 0 0) surfaces after about 3 min and on (1 1 1) surfaces after about 2 min. Fig. 4, which shows the nature of the oxide at short times following anodization in PGT of pH = 9.4 and a current density of $0.16\,mA\,cm^{-2}$ with illumination, yields direct proof that the formation of the oxide layer follows the development of nucleation centres. The increased oxidation rate upon illumination of n-type semiconductors confirms the generally accepted view [8] that positive holes are responsible for the surface reaction in samples that are not heavily doped. A high uniform distribution of nucleation centres leads to a rapid growth of a uniform oxide film as previously observed for n-type GaAs [5].

Our observations on (1 1 1) faces of InP apply also to the n-type quaternary alloys $Ga_xIn_{1-x}As_yP_{1-y}$ ($y \simeq 2x$) grown on (1 1 1) InP substrates. The anodic oxidation in this material is also highly sensitive to pH, current density and illumination and a similar growth mechanism and rate of oxide layer growth is found.

A fuller account of this work including details of the structure and composition of the oxide layers will be published elsewhere.

Acknowledgements

JOW thanks the Royal Society for an equipment grant; PJW acknowledges the support of the SRC

(Case Award) and MAE the British Council for a bursary.

References

1. B. SCHWARTZ, *Crit. Rev. Solid State Sci.* 5 (1975) 609.
2. S. M. SPITZER, B. SCHWARTZ and G. D. WEIGLE, *J. Electrochem Soc.* **122** (1975) 397.
3. H. HASEGAWA, K. FORWARD and H. L. HARTNAGEL, *Electron Lett.* **11** (1975) 53.
4. *Idem, Appl. Phys. Lett.* **26** (1975) 567.
5. H. HASEGAWA and H. L. HARTNAGEL, *J. Electrochem Soc.* **123** (1976) 713.
6. J. O. WILLIAMS, P. J. WRIGHT and A. MABBITT, *Mater. Res. Bull* 12 (1977) 1227.
7. S. SZPAK, *J. Electrochem Soc.* **124** (1976) 107.
8. H. GERISCHER, *Electroanal. Chem. Interfacial Electrochem.* **58** (1975) 263.

Received 17 March
and accepted 20 March 1978.

JOHN O. WILLIAMS
PETER J. WRIGHT
M. A. ELMORSI
Edward Davies Chemical Laboratories,
University College of Wales,
Aberystwyth
SALAH E. MORSI
Department of Chemistry
University of Tanta,
Tanta, Egypt

Cracking in layered composites

The progress of a crack through a body or part of a structure will clearly be affected if local variations in the character of the material occur in the path of the crack. A typical example would be the situation when a crack passes through a two-phased material. But almost equally common is the more macroscopic structural variation represented, for example, by a component that has been case-hardened or similarly surface-treated for whatever purpose. Such a situation might be modelled by considering cracking in a sample consisting of a thick plate of some material to which a thinner plate of a different material has been glued. The parameters that will affect the progress of a crack in such a layered structure are the elastic moduli, fracture toughnesses, and relative thicknesses of the two components. A suitable experimental model might be a layered double cantilever beam (DCB) of the kind shown in Fig. 1, and Atkins and Mai [1] have used the Gurney and Hunt analysis [2] to deduce the cracking load for the simplest case of this kind where the thicknesses and elastic moduli of the two components (and therefore their bending stiffnesses, EI) are equal. The fracture toughnesses of the two materials, which determine their cracking loads for a given crack length, are assumed to be different. Fig. 2 shows how the argument, based on a simple energy conservation concept, is developed. The line, OM_1, represents the load/deflection curve for a DCB sample of the tougher of the two components

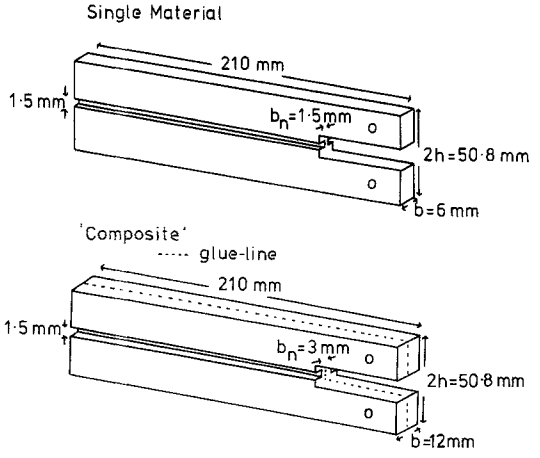

Figure 1 Geometry of double cantilever beam samples.

containing a crack of area A_s. At a critical load P_1 the crack extends in a quasi-static manner and we suppose that when its area reaches A_f the beam is unloaded. In a "reasonably" brittle solid the compliance curve will return to the origin and the fracture work, R_1, can be determined from $OM_1N_1 = R_1(A_f - A_s)$. The cracking of an identical DCB of the less tough material is similarly controlled by the fracture work, R_2, and its Gurney curve is OM_2N_2.

A composite beam containing equal thicknesses of the two materials strongly glued together and tested in the same way will, for the same starting and finishing crack lengths, have compliances identical with those of the two component materials. When the plates are glued together and